https://doi.org/10.1088/2053 1591/aaa604

Elaboration and characterization of $CuInSe_2$ thin films using one-step electrodeposition method on silicon substrate for photovoltaic application

H Saïdi[1], M F Boujmil[1], B Durand[2], J-L Lazzari[3] and M Bouaïcha[1]

[1] Laboratoire de Photovoltaïque, Centre de Recherches et des Technologies de l'Énergie, Technopole de Borj Cédria, Université Tunis El Manar, BP 95, Hammam Lif, 2050 Tunis, Tunisia
[2] CIRIMAT, CNRS, INPT, Université de Toulouse, 118, Route de Narbonne, F 31062 Toulouse cedex 9, France
[3] Aix Marseille Univ, CNRS, CINaM (Centre Interdisciplinaire de Nanoscience de Marseille), Case 913, Campus de Luminy, F 13288 Marseille cedex 9, France

E mail: houdasaiidi@yahoo.fr

Keywords: bifacial solar cell, CIS/c Si, electrodeposition, galvanostatic mode, rapid thermal annealing, heterojunction solar cell

Abstract

Bifacial solar cells combining a heterojunction cell on the upper side and crystalline silicon (c-Si) homojunction on the backside are very interesting devices to a more efficient use of the solar radiation. $Cu(In,Ga)Se_2$(n)/c-Si(p)/c-Si(n^+) or $CuInSe_2$(n)/c-Si(p)/c-Si(n^+) are very attractive heterojunctions to reach this target. In this work, a novel attempt has been made to grow $CuInSe_2$ thin films on p-Si (100) substrate using one-step electrodeposition route with galvanostatic mode. The as-deposited samples were amorphous by nature which implies a rapid thermal annealing step. The effect of annealing temperature on the structural, morphological, optical and electrical properties of the fabricated hetero-structure $CuInSe_2$/c-Si (100) was investigated by x-ray diffraction (XRD), scanning electron microscopy, energy dispersive spectroscopy (EDS) and UV–visible spectroscopy. XRD indicates that $CuInSe_2$ films having single phase chalcopyrite with tetragonal crystal structure are obtained at 350 °C. Values of energy band gap of films at various annealing temperature were estimated to be in the range 0.94–1.01 eV. The optical parameters such as refractive index $n(\lambda)$ and extinction coefficient $k(\lambda)$ were estimated using an appropriate optical model. The AM1.5 current density–voltage characteristic of the fabricated Al/$CuInSe_2$/c-Si (100) hetero-junction solar cell exhibits a short-circuit current density J_{sc} of 4.06 mA cm^{-2}, an open circuit voltage V_{oc} of 0.28 V, a fill factor FF of 36.72% and a solar conversion efficiency η of 0.41%.

1. Introduction

One of the main objectives of scientific research in photovoltaic (PV) is to explore new processing techniques and new materials which assure three criteria; scalability, low-cost and manufacturability. The efficiency of mono-crystalline silicon PV cells has remained nearly unchanged for two decades (current record efficiency being 25.8%) while the module stability is guaranteed over 20 years [1]. A second generation of solar cells based on heterojunction thin film technologies has been developed using scalable manufacturing techniques, non-expensive substrates and alternative materials. Among them copper indium gallium diselenide (CIGS) has shown its full potential in this field [2, 3] since it has a high optical absorption coefficient (~10^5 cm^{-1}), direct band gap and long term optoelectronic stability [4, 5]. CIGS based solar cells (with record efficiency of 22.6%) are now a major candidate for application in building integrated photovoltaics. Correspondingly, silicon HIT heterostructure solar cells, as composed of a mono thin crystalline silicon (c-Si) wafer stacked by ultra-thin amorphous silicon (a-Si) layers, have reached a record efficiency as high as 26.6%. This opens the way for new concepts of heterostructured cells on silicon (Si) combining medium or low band gap materials such as Cu_2ZnSnS_4 (CZTS), a-Si or $CuInSe_2$ (CIS).

A variety of chemical and physical techniques are used to synthesize CIGS films under different experimental conditions, such as co-evaporation [6], spray pyrolysis sputtering [7], pulse laser ablation [8] and electrodeposition [9, 10]. Electrochemical deposition (ECD) is a mature cost-effectiveness method. Its easiness of implementation as a non-vacuum technique makes it suitable for large scale production [11]. Nevertheless, the negative side of ECD is that as-deposited films are amorphous, in best case nano-crystallized. Hence an annealing step is necessary to increase the grain size and to improve crystallinity. In a previous work [12], this problem was solved by annealing electrodeposited CIS films without adding selenium, using rapid thermal process (RTP) during a short time which overcomes the de-selenisation of the layers.

In recent years, many efforts have been devoted to fabricate chalcopyrite absorbing layers by the one-step ECD technique. Obtained results have led to efficiencies of 6%–7% for 30×30 cm^2 surface area and of 10% for laboratory-scale device modules [13]. Many authors have fabricated CIS and CIGS solar cells using a wide variety of substrates such as ITO-coated glass, Mo, Al, Ti, Cu, and polyimide (PI) [14, 15]. Nevertheless, no work to date has been reported on electrodeposition of CIS or CIGS thin films on Si substrates. In addition, comparing to above mentioned works, there is much less work done on p-type Si substrates, except for those using light-assisted electrodeposition of PbSe on p-Si (100) and CdTe on p-Si (111) [16]. Here, it can be noted that the first fabrication and characterization of a heterojunction between bulk CIS and hydrogenated a-Si have been investigated in 1993 by Wu *et al* [17]. In 1994, Tiwari *et al* have reported the characterization of heteroepitaxial $CuIn_3Se_5$ and $CuInSe_2$ layers on Si substrates [18]. More recently, the 'evaporated elemental layers' technique of Cu, In and Se on Si (100) and glass substrates has been studied by Aissaoui *et al* [19]. But no solar cell efficiency has been reported for these heterostructures.

As a result, that remains an interesting challenge to integrate those direct band gap semiconductors with Si technology, so as to achieve heterostructures for bifacial solar cells. More efficient single cells are expected owing to the ability to absorb more of the solar spectrum due to the different band gaps of both materials. The better absorption of CIGS thin film may also help reducing the useful thickness of the monocrystalline silicon wafer. Additionally, this makes possible the realization of bifacial solar cells which could be a combination of an 'upside' heterojunction cell and a 'downside' c-Si homojunction. CIGS (n)/c-Si (p)/c-Si (n+) or CIS (n)/c-Si (p)/c-Si (n^+) are possible architectures to achieve such goal.

In the present study, we report what we believe is the first successful low-cost elaboration and characterization of a heterojunction between CIS and c-Si p-Si (100) using one-step electrodeposition method at constant current density (galvanostatic mode). The focus is to determine the optimal experimental conditions during the ECD and the annealing temperature in order to obtain a high degree of crystallinity and sufficient homogeneity of the CIS films because those are critical parameters for photovoltaic application. The effect of the annealing temperature on the physical properties of ternary CIS films is discussed. The electrical performances of Al/CIS/c-Si (100) heterojunctions are investigated using current density–voltage (J–V) measurements at dark and under AM1.5 illuminations.

2. Experimental details

2.1. Materials preparation

The CIS thin films were electrodeposited on silicon substrates using the galvanostatic mode (at constant current density) with two electrodes system. We used boron doped p-type monocrystalline silicon wafers with a $\langle 100 \rangle$ crystal orientation, a thickness of 525 ± 25 μm and a resistivity in the 1–2 Ω cm range. Before electrodeposition, the silicon wafers were ultrasonically cleaned with acetone, ethanol and de-ionized (DI) water during 10 min. In addition, the Si substrates were then dipped into dilute hydrofluoric acid (HF, 5%) solution for one minute to remove native oxide and obtain a hydrophobic surface. This step of removing the native SiO_2 insulating film is crucial to permit the electrodeposition of CIS on the silicon substrate. Furthermore, since CIS films are successfully electrodeposited on silicon substrate with a good adhesion, no insulating SiO_2 film was left on silicon and the reaction of silicon with the electrolyte to form such oxide layer is weakly probable.

The electrodeposition technique has been carried out using a potentiostat—galvanostat connected to the two-electrodes' cell. The compact potentiostat—galvanostat (Volta Lab PGP 201) using a built-in signal generator can be used as a stand-alone instrument when it is programmed. With the Volta Master 4 software, we can easily control the current, the duration and the cycle's number of the ECD. The working electrode was a silicon substrate with a surface area of 2.5 cm^2 and platinum was used as a counter electrode. For the growth of CIS thin films under galvanostatic mode, a constant current density of 10 mA cm^{-2} was applied and the optimized deposition time was 10 min.

The composition of the electrolytic solutions consisted of 0.003 M of $CuCl_2$, 0.003 M of $InCl_2$, 0.008 M of SeO_2 and 0.1 M of sodium citrate which was chosen to be a complexing agent in DI water. The pH of the bath was maintained at 1.65 by the addition of HCl and the solution was stirred during deposition. The thermal

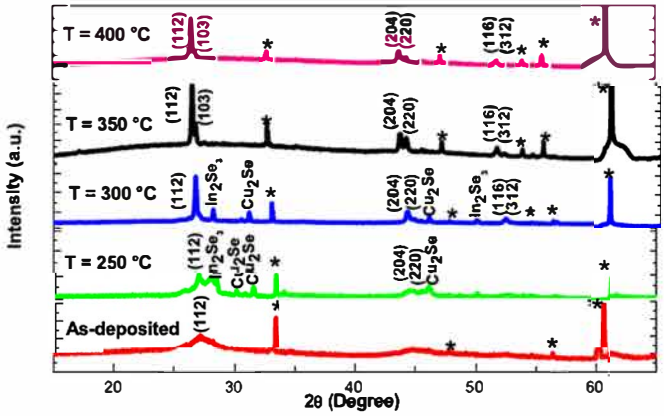

Figure 1. XRD patterns of electrodeposited CIS films on Si (100) substrate as a function of the annealing temperature. The peaks associated with Si (100) are highlighted by (*).

Table 1. Structural parameters of the as synthesized and annealed CIS films with RTP at various annealing temperatures.

Annealing temperature T (°C)	Bragg angle (°)	FWHM (°)	Grain size D (nm)	Lattice constants (Å)		
				a	c	Strain ($\varepsilon \times 10^{2}$)
As deposited	26.88	1.05	8.0	5.730	11.511	1.900
250	26.68	0.17	46.0	5.751	11.595	0.304
300	26.74	0.14	58.0	5.770	11.474	0.250
350	26.45	0.12	67.3	5.775	11.500	0.206
400	26.44	0.11	73.4	5.776	11.505	0.203

annealing of the as-deposited CIS films was carried out in a nitrogen atmosphere at temperature in the range of 250–400 °C for 5 min by RTP using IR heating lamps.

2.2. Characterization

Structural characterization of the fabricated CIS thin films was done by XRD analysis in 2θ mode (10°–70° angle range) using an automated Bruker D8 advanced diffractometer and the CuK_{α} ($\lambda = 1.540$ Å) radiation. The reflectance spectra $R(\lambda)$ of the electrodeposited CIS films was measured at room temperature by a UV–visible-NIR LAMBDA 950 spectrophotometer for wavelengths ranging between 350 and 2000 nm. Surface cross-sectional morphologies of the samples were observed by a scanning electron microscope (SEM) JEOL JSM-5910, with an accelerating voltage of 20 kV. In addition, their compositions were determined by EDS.

Heterojunction solar cells with an active area of about 0.78 cm^2 have been fabricated using conventional photolithography technique. Back and grid front aluminum (Al) contacts were deposited by thermal evaporation followed by an annealing step. J–V characteristics were measured by a digital source meter (Keithley Instruments Inc., Model 2400) in the dark and under AM1.5 (100 mW cm^{-2}) illumination.

3. Results and discussion

3.1. Structural analysis

XRD patterns recorded for CIS thin films grown on Si (100) substrates under different RTP annealing temperature of 250 °C, 300 °C, 350 °C and 400 °C are depicted in figure 1. According to the width of XRD peaks, one guess that the grains' size of the as-deposited CIS layers is very small, e.g. those layers are amorphous. A low crystallization appears for CIS film treated at 250 °C. When we increase the annealing temperature, the peaks corresponding to (112), (103), (204), (220), (116) and (312) plans of the well-identified CIS chalcopyrite phase (Reference JCPDS 40-1487) appear. In addition, secondary phases of Cu_2Se and In_2Se_3 are observed for annealing temperature of 250 °C, but those binary phases are not detected above 300 °C. Several investigations [20, 21] have proved that the formation of $CuInSe_2$ is produced from the reaction between Cu_2Se and In_2Se_3. Upon heat treatment at 350 °C, a single chalcopyrite structure phase is obtained with a strong and preferential orientation along the (112) direction. Similar (112) peak has also been observed for $CuInSe_2$ films synthesized on Si (100) wafers [19]. As reported in table 1, the full width at half maximum (FWHM) of the main (112) peak is

Table 2. The elemental composition of EDS patterns of CIS thin films at different annealing temperature.

		Atomic ratio (%)	
Annealing temperature T (°C)	Cu	In	Se
250	21.92	13.81	64.26
300	29.41	17.47	53.11
350	26.14	22.83	51.03
400	28.42	23.33	48.25

found to decrease from 612 to 396 arc seconds with an increase in annealing temperature from 250 °C to 400 °C. This indicates that the crystalline nature of the samples improves when the RTP annealing temperature rises. Improved crystallinity was verified through the change in grain sizes, which were estimated from the highest peak intensity by the Scherrer's formula expressed as equation (1) [22, 23].

$$D = \frac{k\lambda}{\beta \cos \theta}, \tag{1}$$

where λ is the wavelength of CuKα line ($\lambda = 1.540$ Å), θ is the Bragg angle, β is the values of the FWHM of the (112) peak and k is a constant usually taken equal to 0.9. The calculated values of the crystallite size are given in table 1. The largest crystallites with mean grain diameters of 67 and 73 nm are obtained at 350 °C and 400 °C, respectively. Improvement of the crystallization is observed when the annealing temperature reaches 350 °C.

In table 1, one can also note a small shift of the (112) peak to lower angle for temperatures of 350 °C and 400 °C. This can be due to a better relaxation of the strain related to the in-plane lattice mismatch (6.0%) between CIS ($a = 5.78$ Å) and Si (5.45 Å). The lattice constants for CIS films assuming tetragonal symmetry are calculated using the following formula:

$$\frac{1}{d^2{}_{hkk}} = \frac{h^2 + k^2}{a^2} + \frac{l^2}{c^2}, \tag{2}$$

where $d_{(hkl)}$ is the inter-plane spacing. The two lattice parameters a and c are given in table 1. They range from 5.730 to 5.776 Å and 11.474 Å to 11.595 Å, respectively. These values are in good agreement with those indicated in the JCPDS reference files [24]. The micro-strain ε was evaluated using the following relation [25]:

$$\varepsilon = \frac{\beta}{4 \tan \theta}. \tag{3}$$

It is known that the micro-strain ε affects the optoelectronic properties of the films due to the distorted lattice. Values of ε decreases from 1.9% for as-deposited sample to 0.2% for sample annealed at 350 °C. This is attributed to the reduced level of defect and grain boundaries due to increased grain size. Hence, annealing temperature of 350 °C appears necessary for the formation of films with good structural quality.

3.2. Morphological and compositional analysis

The surfaces morphologies of the electrodeposited CIS displayed in figure 2 were investigated by SEM. The latter shows that the annealing temperature affects the morphology of the films by changing the particles size. In fact, micrograph of figure 2(a) shows non-homogeneous surface composed of grains with non-uniform distribution. When the annealing temperature reaches 350 °C (figure 2(d)), we notice a reduction of the size of the clusters leading to a homogenous surface. The grain' size distribution appears to be relatively uniform with a mean crystallite size varying between 100 and 400 nm. Grains seen under SEM may contain several individual nanocrystals (NCs). This could explain the difference in values of crystallite size calculated from XRD data (about 70 nm) and those deduced from SEM micrographs. Otherwise, for the film treated at 400 °C, much larger grains appear while the surface morphology is more disordered (figure 2(e)).

Figure 2(f) provides a typical cross-sectional SEM image of the CIS film grown on Si (100) after annealing at 350 °C. The deduced film thickness is around 3 μm, the layer looks dense, but the surface profile reveals a strong micrometer scale roughness. Such roughness is incompatible with imaging by atomic force microscopy leading to overestimated root mean squared roughness (rms) of 0.79 μm for the as-deposited sample. The surface profiles have been studied using a DEKTAK-XT profilmeter over scan length of 300 μm with a stylus force of 1 mg and a scan speed of 10 μm s^{-1}. The radius of curvature of the tip is 2 μm. The rms were found to be 0.83 μm for the as-deposited sample and 0.70 μm, 0.64 μm, 1.10 μm and 1.06 μm for samples annealed at 250 °C, 300 °C, 350 °C and 400 °C, respectively. Those values agree with SEM morphologies observed in insert of figures 2(a)–(e).

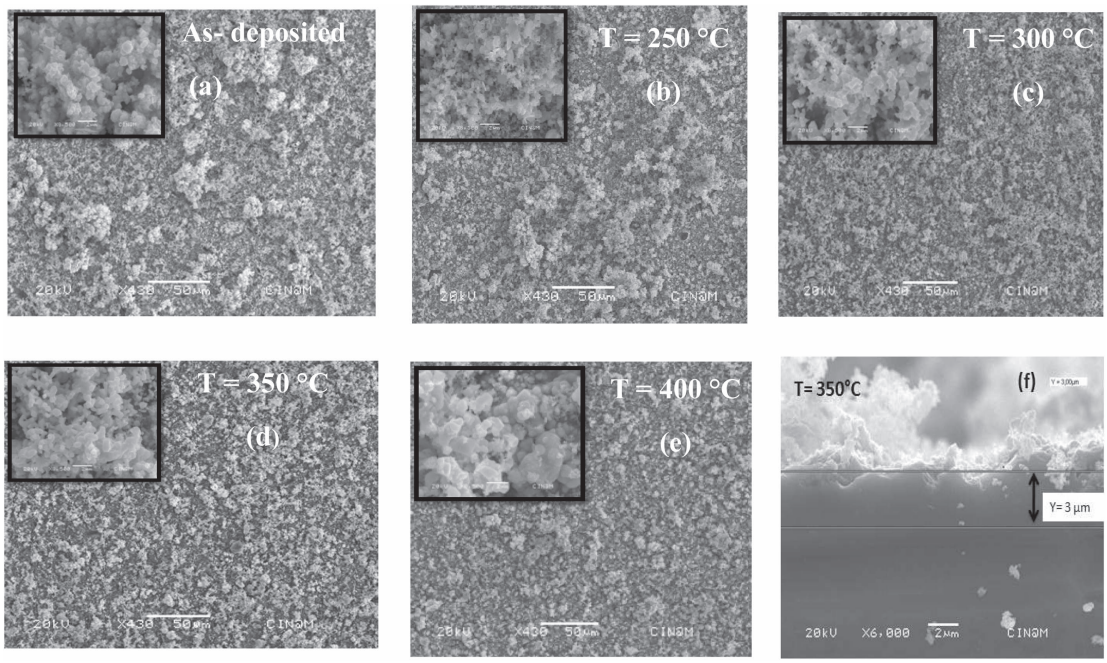

Figure 2. SEM images of top surface and cross section of electrodeposited CIS layers on Si (100) before and after annealing using RTP furnace: (a) before annealing; (b) (e) annealed at 250 °C, 300 °C, 350 °C and 400 °C, respectively; (f) SEM cross section of simple annealed at 350 °C.

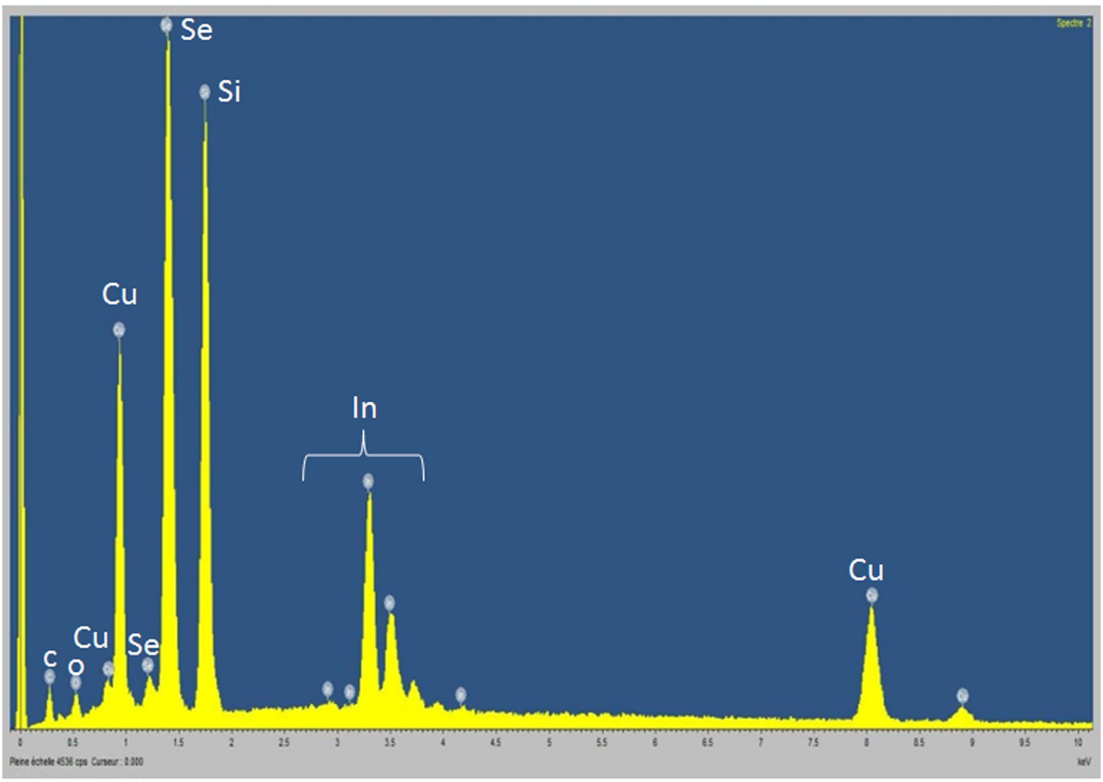

Figure 3. The composition analysis obtained by EDS of the CIS film annealed at 350 °C.

Figure 3 shows a typical EDS spectrum for sample annealed at 350 °C that reveals the presence of copper, indium and selenium elements. Silicon is likely attributed to the substrate. Other elements such as residual oxygen and carbon may be due to surface and interface contaminations. The compositional analysis of those CIS films is summarized in table 2. We note that the best stoichiometry in at% is obtained for CIS film annealed at

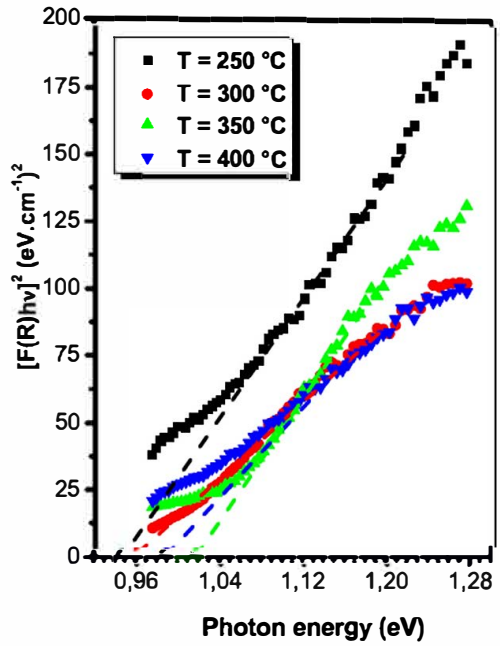

Figure 4. Plot of $(F(R)\,h\nu)^2$ versus $(h\nu)$ using a Kubelka Munk approximation for CIS films deposited on silicon substrate at different annealing temperatures.

350 °C with no loss in Selenium. From the above results obtained by XRD, SEM and EDS analysis, it appears that samples annealed at 350 °C have improved crystallization properties.

3.3. Optical properties

The optical band gaps of layers annealed at 250 °C, 300 °C, 350 °C and 400 °C were estimated in order to determine which one presents the absorption edge closest to that of stoichiometric CIS semiconductor. Several investigations [26, 27] have reported methods to determine the absorption coefficient of electrochemically or -vacuum deposited thin films on non-absorbing substrates from measurements of light reflectance. But in this case, it is difficult to evaluate the absorption coefficient of these films using the Lambert–Beer law. Hence, the total reflection spectra (specular and diffusion) were recorded using an integrated sphere on different spots for each film to minimize the error of missing the diffused component of the reflected beam. Besides, it is well-known that CIS is a direct band gap semiconductor which can be estimated from the linear absorption coefficient, α, according to Tauc's formula [28]:

$$\alpha h\nu = A_0\,(h\nu - E_g)^{1/2}, \tag{4}$$

where $h\nu$ is the incident photon energy, A_0 is a constant and h is the Planck constant.

The absorption coefficient could be approximated using the Kubelka–Munk function $F(R)$, defined with respect to reflectivity of dense samples ($R = R_\infty$) through the following equation:

$$F(R) = \frac{(1 - R)^2}{2R}. \tag{5}$$

The optical band gap of CIS films has been calculated by plotting $[F(R)\,h\nu]^2$ versus $h\nu$ as illustrated in figure 4, where we extrapolate the straight line- portion of the absorption edge to find the intercept with energy axis. We found that the band gap energy value increases from 0.94 to 1.01 eV when the annealing temperature rises. We also note that the sample annealed at 350 °C have larger band gap (1.01 eV) than that one annealed at 400 °C (0.98 eV). In general, higher values of the optical band gaps are assigned to less intrinsic and extrinsic defects which give less contribution below the absorption edge. Similar result was shown by other studies [29, 30]. An optimum value of $E_g \sim 1.01$ eV is likely with the formation of a single ternary CIS phase.

3.4. Optical modeling

A fitting program written in Mathlab was used in order to extract the optical parameters such as the refractive index, $n(\lambda)$, the extinction coefficient $k(\lambda)$ and the band gap energy from experimental curves of reflectivity $R(\lambda)$. We used the Fresnel matrix method applied to CIS thin films where we consider two consecutive layers in contact with air, e.g. an air/$CuInSe_2$/Si(100)/air stacking. Both layers have complex refractive indexes and thicknesses ($\tilde{n}_1$, d_1) and ($\tilde{n}_2$, d_2), respectively. The refractive index in air is noted n_0. More detailed information

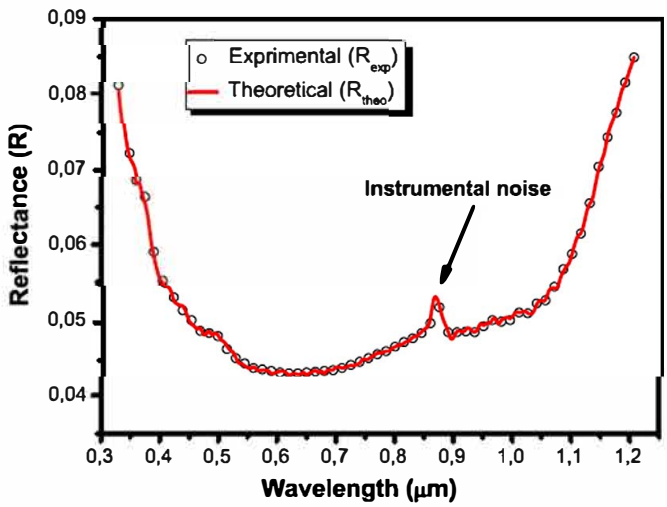

Figure 5. Fitting results of theoretical $R_{theo}(\lambda)$ and experimental $R_{exp}(\lambda)$ reflectance spectra of CIS film after RTP annealing at 350 °C. The instrumental noise is due to an automatic change of detectors in the UV vis NIR spectrophotometer apparatus.

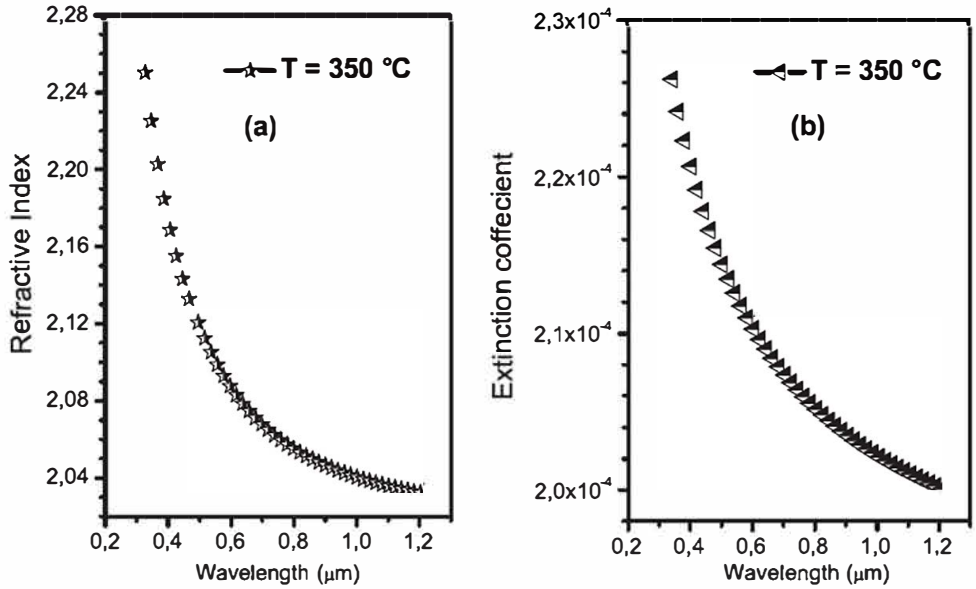

Figure 6. Optical parameters: (a) refractive index, n, and (b) extinction coefficient, k, versus wavelength for $CuInSe_2$ thin films treated at 350 °C.

on calculation methods using Fresnel matrix within this model are reported in our previous work [12]. The theoretical values of optical parameters were determined using the *Cauchy* model according to the following equations:

$$n = A + \frac{B}{\lambda^2} + \frac{C}{\lambda^4}, \tag{6}$$

$$k = \frac{D}{\lambda} + \frac{E}{\lambda^3} + \frac{F}{\lambda^5}, \tag{7}$$

where λ is the wavelength and A, B, C, D, E and F are constants. By fitting theoretical curve of $R(\lambda)$ to experimental one over the entire spectral range [300–1300 nm] as plotted in figure 5, we can determine the band gap energy, the refractive index, n, and the extinction coefficient, k, of all films. Thereby, the best fitting result was obtained for the CIS film after RTP annealing at 350 °C.

Figures 6(a) and (b) show the variation in extinction coefficient and refractive index as a function of the wavelength for CIS film treated at 350 °C, which reveals a decreasing in refractive index and extinction coefficient with increasing wavelength. Values of n and k reach 2.03 and 2.0 10 ^{4}, respectively, in the near infrared range.

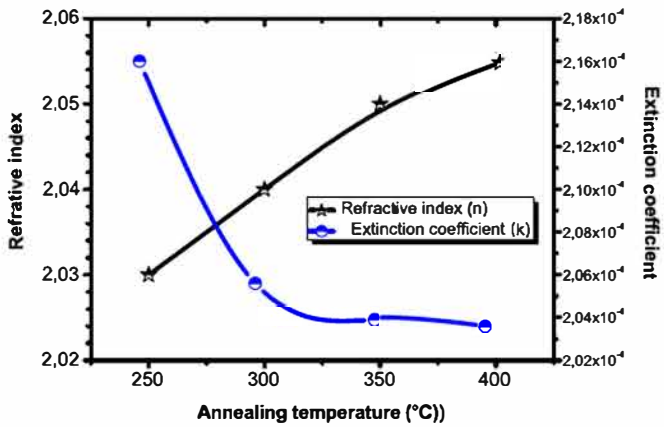

Figure 7. Variation of the refractive index and the extinction coefficient of CIS films as a function of annealing temperature at set wavelength λ 1100 nm.

The effect of annealing temperature on the optical constants of CIS films are illustrated in figure 7 for a fixed wavelength of 1100 nm. The refractive index rises when the annealing temperature increases to a value of 2.055 for films heated at 400 °C. This could be explained by a densification of the films after annealing. In contrast, the extinction coefficient decreases considerably with annealing temperature, reaching a value of about 2.04×10^{-4} for film annealed in the 350 °C–400 °C range. These results indicate the formation of a single CIS chalcopyrite phase above 350 °C. The band gap energy was estimated from the absorption coefficient according to the following equation:

$$\alpha = \frac{4\pi k}{\lambda}. \tag{8}$$

Values of the optical band gap E_g of CIS layers as a function of annealing temperature are shown in figure 8. The samples exhibit a gradual shift in the optical spectra towards higher energies. These band gaps range from 0.92 to 1.07 eV when the annealing temperature rises. These values are in good agreement with those deduced from the reflection spectra. The lower values of E_g obtained at 250 °C and 300 °C could be due to absorption by impurity or by the In_2Se_3 secondary phase.

3.5. Current density–voltage characterization

Highly polycrystalline CIS thin films were obtained using one-step electrodeposition upon galvanostatic mode on silicon substrate followed by RTP annealing at 350 °C. For front grid and back contacts, we thermally evaporate aluminum. The typical J–V characteristics of the fabricated Al/CIS/Si (100) heterojunction under dark and AM1.5 illumination are plot in figure 9. One can notice the rectifying behavior of this heterojunction under dark. Values of serial R_s and shunt R_{sh} resistances are 2 Ω and 1000 Ω, respectively. These values are very interesting for such heterojunction solar cell. They indicate low recombination (R_s) and low leakage current (R_{sh}). The cell exhibits a short circuit current density J_{SC} of 4.06 mA cm^{-2}, an open circuit voltage V_{OC} of 0.28 V, a fill factor FF of 36.72% and a power conversion efficiency η of 0.41%.

V_{OC} and J_{SC} are much lower than the ones obtained for solar cells fabricated by others cost-effective techniques in [31, 32]. However, similar poor efficiency of 0.3% was obtained by Jin *et al* [33] with heterojunctions based on $CuInSe_2$ NCs/CdS quantum dots (QDs)/ZnO nanowire (NW) arrays. It is generally assumed that low FF are related to charge percolation in nanostructured materials such as CIGS, NCs, NWs or QDs. The low J_{SC} may arise from a strong recombination of the photo-carriers at surface and interface states. The low V_{OC} value is surprising. It could be due to a compositional band gap narrowing of CIS layer at the interface or to a type II CIS/Si tunneling interface.

Further works could improve the cell performances through (i) optimizing the physicochemical surface preparation of the silicon substrate, (ii) a mechanical chemical polishing of CIS layers, (iii) a surface passivation of CIS nanocrystallites, (iv) the use of a transparent conductive oxide deposited in a conformal way by atomic layer deposition, or (v) through the incorporation of Ga into the absorber to increase the band gap energy. For that purpose, an accurate study of the chemical bonding should be done by x-ray photoemission spectroscopy at each step of process.

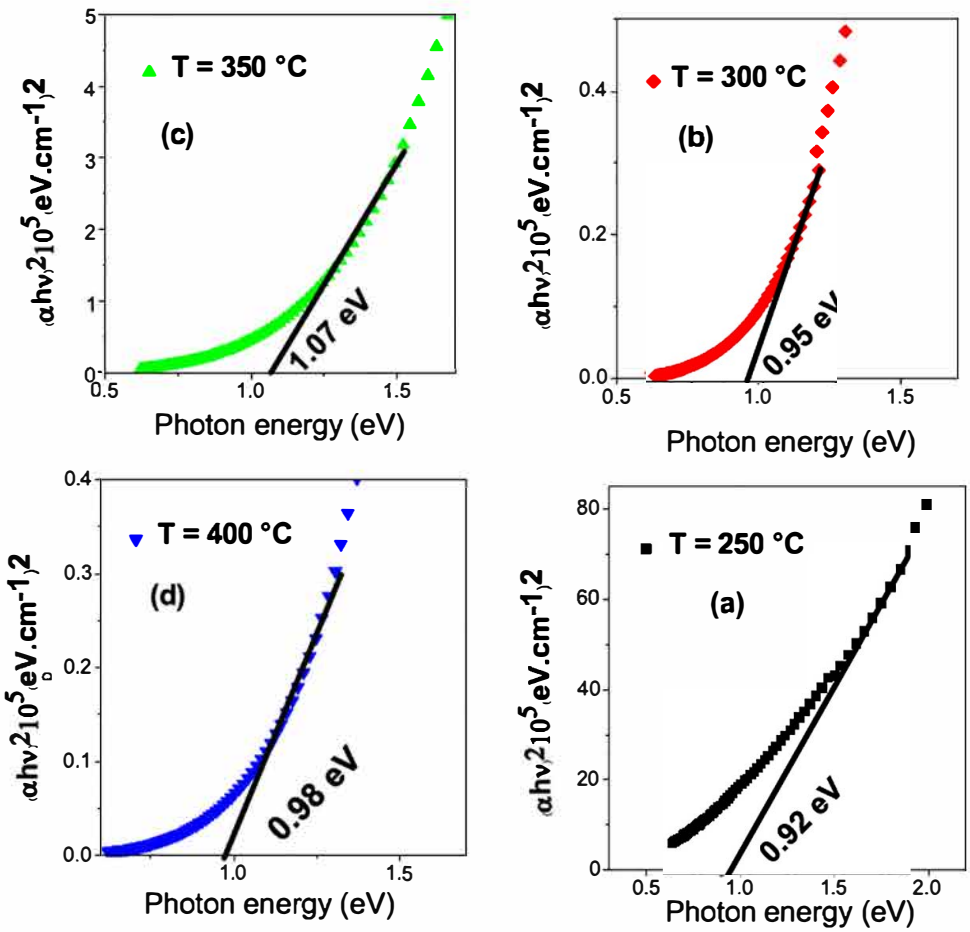

Figure 8. Plots of $(\alpha h\nu)^2$ versus photon energy ($h\nu$) using optical modeling for CIS films on silicon substrate at various annealing temperatures.

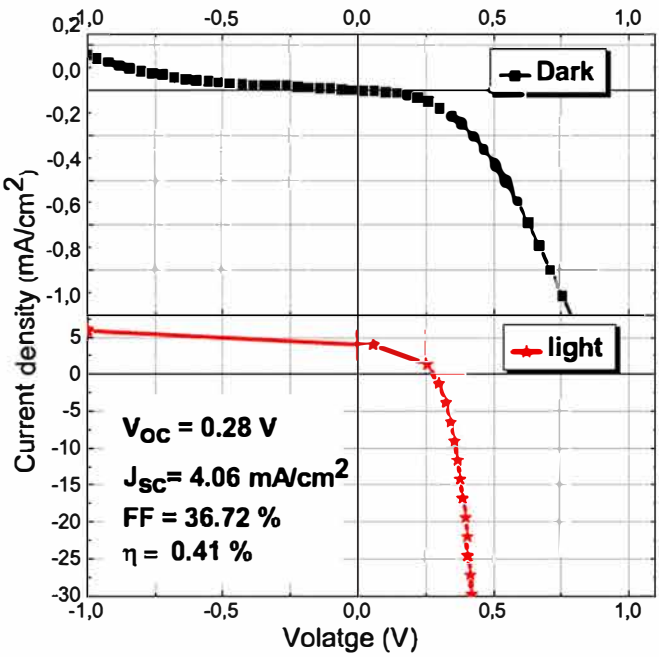

Figure 9. Dark and light J V curves of the fabricated Al/CIS/c Si/Al hetero junction using the sample annealed at 350 °C.

4. Conclusion

In summary, a galvanostatic electrodeposition method was successfully employed to deposit $CuInSe_2$ thin films on monocrystalline Si (100) substrates. The as-deposited films are amorphous thus requiring RTP heat treatment. The effect of annealing temperature on physicochemical proprieties of CIS films was investigated by XRD, SEM and EDS analysis. We pointed out the formation at 350 °C of nanocrystalline layers of single phase stoichiometric CIS with preferential orientation along (112) direction.

The optical modeling showed that the refractive index and the extinction coefficient in the near infrared region ($\lambda = 1100$ nm) are greatly influenced by the annealing temperature. The optical band gap measured by UV–visible-IR reflectance is about 1.01 eV which is close to that calculated by optical modeling of theoretical spectra (1.07 eV).

The electrical characteristics of CIS/c-Si based heterojunction solar cell were assessed by J–V measurements under dark and AM1.5 illumination. A 36.72% fill factor, a 4.06 mA cm^{-2} short circuit current density, a 0.28 V open circuit voltage, and a 0.41% power conversion efficiency were obtained. These poor performances may be explained by percolation of the photo-carriers to the Al contact surface and to CIS/Si interface followed by a strong recombination at defect states. Capacitance–voltage spectroscopy may help to understand the origin of the low value of V_{oc}. The minority carrier lifetime should be adressed as well.

Nevertheless, this novel one step electrodeposition approach has proved being successful to fabricate a heterojunction cell between a nanocrystalline $CuInSe_2$ film and a monocrystalline silicon substrate. Although perfectible, this simple process allows an easy control of the chemical composition of CIS layers, and could be applicable to produce CIS based solar cell and modules.

Acknowledgments

Authors would like to thank Vasile Heresanu, Damien Chaudanson, Alain Ranguis and Frédéric Bedu from the Centre Interdisciplinaire de Nanoscience de Marseille for their fruitful help in characterization of CIS samples by XRD, SEM, EDS, AFM and surface profilometry, respectively.

ORCID iDs

M Bouaïcha https://orcid.org/0000-0002-6294-2541

References

[1] Compaan A D 2006 Photovoltaics: clean power for the 21st century *Sol. Energy Mater. Sol. Cells* 90 2170 80
[2] Téllez H, Druce J, Hall A, Ishihara T, Kilner J and Rockett A 2015 Low energy ion scattering: surface preparation and analysis of $Cu(In,Ga)Se_2$ for photovoltaic applications *Prog. Photovolt. Res. Appl.* 23 1219 27
[3] Jackson P, Hariskos D, Lotter E, Paetel S, Wuerz R and Menner R 2011 Polycrystalline $Cu(InGa)Se_2$/CdS thin films solar cells made by new precursors *Prog. Photovolt., Res. Appl.* 19 894 7
[4] Maeda T, Takeichi T and Wada T 2006 Systematic studies on electronic structures of $CuInSe_2$ and the other chalcopyrite related compounds by first principles calculations *Phys. Status Solidi a* 203 2634 8
[5] Duchatelet A, Sidali T, Loones N, Savidan G, Chassaing E and Lincot D 2013 12.4% Efficient Cu (In,Ga)Se_2 solar cell prepared from one step electrodeposited Cu In Ga oxide precursor layer *Sol. Energy Mater. Sol. Cells* 119 241 5
[6] Contreras M A, Romero M J and Noufi R 2006 Characterization of Cu(In,Ga)Se_2 materials used in record performance solar cells *Thin Solid Films* 51 511 2
[7] Krunks M, Kijatkina O, Rebane H, Oja I, Mikli V and Mere A 2002 Composition of $CuInS_2$ thin films prepared by spray pyrolysis *Thin Solid Films* 403 404 71 5
[8] Mustfa H, Hunter D, Pradhan A K, Roy U N, Cui Y and Burger A 2007 Synthesis and characterization of $AgInSe_2$ for application in thin film solar cells *Thin Solid Films* 515 7001 4
[9] Wellings J S, Samantilleke A P, Heavens S N, Warren P and Dharmadasa I M 2009 Electrodeposition of $CuInSe_2$ from ethyleneglycol at 150 °C *Sol. Energy Mater. Sol. Cells* 93 1518 23
[10] Mandati S, Sarada B V, Dey S R and Joshi S V 2013 Pulsed electrodeposition of $CuInSe_2$ thin films with morphology for solar cell applications *J. Electrochem. Soc.* 160 173 7
[11] Meglali O, Attaf N, Bouraiou A, Bougdira J, Aida M S and Medjahdi G 2014 Chemical bath composition effect on the properties of electrodeposited $CuInSe_2$ thin films *J. Alloys Compd.* 587 303 7
[12] Saidi H, Boujmil M F, Durand B and Bouaïcha M 2017 Physical properties of highly crystalline CIS layer prepared using single phase electrodeposition and low temperature RTP annealing *J. Alloys Compd.* 695 779 86
[13] Taunier S *et al* 2005 Cu(In,Ga)(S,Se)$_2$ solar cells and modules by electrodeposition *Thin Solid Films* 480 481 526 31
[14] Kessler F and Rudmann D 2004 Technological aspects of flexible CIGS solar cells and modules *Sol. Energy* 77 685 95
[15] Otte K, Makhova L, Braun A and Konovalov I 2006 Flexible Cu(In,Ga)Se_2 thin film solar cells for space application *Thin Solid Films* 511 512 613 22
[16] Ivanou D K, Streltsov E A, Fedotov A K, Mazanik A V, Fink D and Petrov A 2005 Electrochemical deposition of PbSe and CdTe nanoparticles on top Si (100) wafers and into nanopores in SiO_2/Si(100) structure *Thin Solid Films* 490 154 60
[17] Wu S and Haneman D 1993 Heterojunctions of $CuInSe_2$ with amorphous hydrogenated silicon *Appl. Phys. Lett.* 73 265

[18] Tiwari A N, Blunier S, Filzmoser M, Zogg H, Schmid D and Schock H W 1994 Characterization of heteroepitaxial $CuIn_3Se_5$ and $CuInSe_2$ layers on Si substrates *Appl. Phys. Lett.* **65** 3347
[19] Aissaoui O, Mehdaoui S, Bechiri L, Benabdeslem M, Benslim N, Amara A, Mahdjoubi L and Nouet G 2007 Synthesis and material properties of Cu III VI_2 chalcopyrite thin films *J. Phys. D: Appl. Phys.* **40** 5663 5
[20] Deng W, Yan Z, Ding P, Wang Y, Fang Y, Su M and Su Y 2014 Phase composition of $CuInSe_2$ in different annealing process *Mater. Sci. Semicond. Process.* **26** 419 24
[21] Papadimitriou D, Roupaka G, Sáez Araoz R, Lux Steiner M C, Nickel N H, Alamé S, Vogt P and Kneissl M 2015 Quality $CuInSe_2$ and $Cu(In,Ga)Se_2$ thin films processed by single step electrochemical deposition techniques *Mater. Res. Express* **2** 056402
[22] Faraday M 1834 Experimental researches in electricity. Seventh series *Phil. Trans. R. Soc.* **124** 77
[23] Weast R C (ed) 1980 *CRC Handbook of Chemistry and Physics* (Boca Raton, FL: CRC Press)
[24] Fons P, Niki S, Yamada A, Uchino M and Oyanagi H 2000 *Copyright © JCPDS International Centre for Diffraction Data, Advances in X ray Analysis* 43, 201 11
[25] Vanheusden K, Seager C H, Warren W L, Allant T D R and Voigt J A 1996 Correlation between photoluminescence and oxygen vacancies in ZnO phosphors *J. Appl. Phys. Lett.* **68** 403 5
[26] Zarpellon J, Jurca H F, Klein J J, Schreiner W H, Mattoso N and Mosca D H 2002 Electrodeposition of Fe thin films on Si (111) surfaces in the presence of sodium saccharin *Electrochim. Acta* **53** 2002 8
[27] Tuttle J R, Albin D S, Matson R J and Noufi R 1989 A comprehensive study on the optical properties of thin film $CuInSe_2$ as a function of composition and substrate temperature *J. Appl. Phys.* **66** 4408 17
[28] Guillén C and Herrero J 1991 Optical properties of electrochemically deposited $CuInSe_2$ thin films *Sol. Energy Mater.* **23** 31 452
[29] Zouaghi M C, Nasrallah T B, Marsillac S, Bernèd J C and Said B 2001 Physicochemical characterization of spray deposited $CuInS_2$ thin films *Thin Solid Films* **39** 46 382
[30] Koutsikou R and Bouroushian M 2015 Pulse potential electrodeposition of (112) textured chalcopyrite $CuInSe_2$ films from acidic aqueous solutions *Electrochim. Acta* **178** 856 70
[31] Pathak D, Bedi R K and Kaur D 2010 Growth of heteroepitaxial $AgInSe_2$ layers on Si (100) substrates by hot wall method *Optoelectron. Adv. Mater.* **4** 657 61
[32] Liu W, Mitzi D B, Yuan M, Kellock A J, Chey S J and Gunawan O 2010 12% efficiency $CuIn(Se,S)_2$ photovoltaic device prepared using a hydrazine solution process *Chem. Mater.* **22** 1010 4
[33] Guo Q J, Kim S J, Kar M, Shafarman W N, Birkmire R W, Stach E A, Agrawal R and Hillhouse H W 2008 Development of $CuInSe_2$ nanocrystal and nanoringinks for low cost solar cells *Nano Lett.* **8** 2982 7